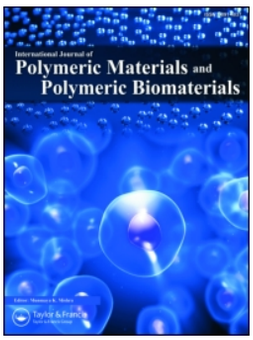

International Journal of Polymeric Materials and Polymeric Biomaterials

ISSN: 0091-4037 (Print) 1563-535X (Online) Journal homepage: https://www.tandfonline.com/loi/gpom20

Poly(L-lactide-*co*-caprolactone)/collagen electrospun mat: Potential for wound dressing and controlled drug delivery

C. R. Reshmi, Tara Menon, Anupama Binoy, Nandita Mishra, K. K. Elyas & A. Sujith

To cite this article: C. R. Reshmi, Tara Menon, Anupama Binoy, Nandita Mishra, K. K. Elyas & A. Sujith (2017) Poly(L-lactide-*co*-caprolactone)/collagen electrospun mat: Potential for wound dressing and controlled drug delivery, International Journal of Polymeric Materials and Polymeric Biomaterials, 66:13, 645-657, DOI: 10.1080/00914037.2016.1252357

To link to this article: https://doi.org/10.1080/00914037.2016.1252357

View supplementary material

Published online: 02 May 2017.

Submit your article to this journal

Article views: 238

View related articles

View Crossmark data

Citing articles: 8 View citing articles

Full Terms & Conditions of access and use can be found at
https://www.tandfonline.com/action/journalInformation?journalCode=gpom20

INTERNATIONAL JOURNAL OF POLYMERIC MATERIALS AND POLYMERIC BIOMATERIALS
2017, VOL. 66, NO. 13, 645–657
http://dx.doi.org/10.1080/00914037.2016.1252357

Taylor & Francis
Taylor & Francis Group

Poly(L-lactide-*co*-caprolactone)/collagen electrospun mat: Potential for wound dressing and controlled drug delivery

C. R. Reshmi[a], Tara Menon[b], Anupama Binoy[c], Nandita Mishra[c], K. K. Elyas[b] and A. Sujith[a]

[a]Material Research Laboratory, Department of Chemistry, National Institute of Technology Calicut, Calicut, India; [b]Department of Biotechnology, University of Calicut, Calicut, India; [c]School of Biotechnology, Amrita Vishwa Vidyapeetham, Kollam, India

ABSTRACT

Here we report a novel bioactive electrospun mat based on poly(L-lactide-*co*-caprolactone) (PLLC) and collagen for wound dressing and sustained drug delivery of gentamicin. PLLC/collagen electrospun mat loaded with 10% gentamicin showed bioactivity for 15 days against Gram-positive and Gram-negative bacteria. The *in vitro* cell culture of 3T3 fibroblasts confirmed that these electrospun mat provide an increased specific interface area and hydrophilicity to enhance cell attachment, proliferation, and migration. The modified PLLC/collagen mat provided an excellent enhancement in properties of antibacterial wound dressings with a minimum *in vitro* toxicity and high potency for promoting wound healing stages.

GRAPHICAL ABSTRACT

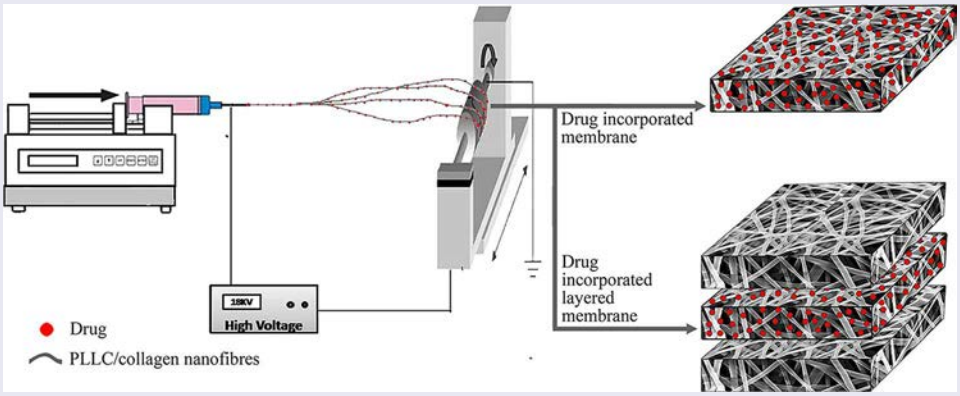

ARTICLE HISTORY
Received 30 July 2016
Accepted 17 October 2016

KEYWORDS
Collagen; controlled drug delivery; electrospinning; poly(L-lactide-*co*-caprolactone); wound dressing

1. Introduction

Wound dressing and tissue engineering materials embedded with therapeutic drugs is an interdisciplinary field and have an important role in biomedical and pharmaceutical research. Bacterial infection beneath the wound dressing was the major challenge faced during the treatment of wounds which results in scar formation, disfiguring, or even threaten to life [1]. Repeated replacement of wound dressing and antibiotics cause damage to newly formed epithelial tissues and delays wound healing [2]. Conventional wound dressing materials cannot meet the requirements for rapid wound healing, because of the disadvantages such as adherence to wound, burst release of antibiotics, insufficient water, and air permeation. Therefore, fabrication of a wound dressing material which overcomes the above disadvantages and performs sustained drug releasing kinetics attracts biomedical researcher's interest. Biological [3], biochemical [4–6], and polymeric [7–9] bandages gained much attention to rectify these problems.

Electrospun polymer nanofibrous mats are an emerging area in biomedical field, which can be widely applicable in wound dressing [10,11], tissue engineering [12], and controlled drug delivery [13,14]. Electrospun fibers are regarded as a very promising bioactive novel wound healing platform because of its very fine nanometer diameter, high surface-to-volume ratio, porosity, hemostatic properties, flexibility, absorbability, and semipermeability. These properties improve the respiration of cells, provide better conformation to the wound surface, and it also helps drug particles to diffuse out of the matrix efficiently [15–17]. Electrospun mats resemble the functions of extracellular matrix (ECM) and it enhances restoration, proliferation, and migration of epithelial cells toward the wound sites. During these years, polymers used

CONTACT A. Sujith athiyanathil.sujith@gmail.com Material Research Laboratory, Department of Chemistry, National Institute of Technology Calicut, Calicut, Kerala 673601, India.
Color versions of one or more of the figures in this article can be found online at www.tandfonline.com/gpom.
Supplemental data for this article can be accessed on the publisher's website.
© 2017 Taylor & Francis

for controlled and specific drug delivery to wounds include poly(lactide-*co*-glycolide) (PLGA) [18], poly(vinyl pyrrolidone) [19], poly(vinyl alcohol) [20], poly(hydroxyalkylmethacrylates) [21], polyurethane [22], poly(lactic acid) (PLA) [23], poly(caprolactone) (PCL) [24–26], chitosan [27], and alginate [28]. The main advantage of electrospun wound healing system is that it offers site-specific drug delivery and can avoid drug accumulation in internal organs which cause serious health issues. The electrospun biodegradable polymeric mats also act as a barrier layer for bacterial penetration and provides a better platform for water, fluid, and air permeation. New human epithelial layer can attach and organize well around the nanofibers consequently the highly biodegradable electrospun nanofibers degrade off, and the risk of repeated application of wound dressing can be avoided.

In the present study, poly(L-lactide-*co*-ε-caprolactone) (PLLC) and collagen are the polymers selected to fabricate electrospun wound dressing material. PLLC is a biocompatible copolymer of PCL and PLA. PLLC is a biocompatible polymer approved by FDA and shows unique elastic properties and biocompatibility [29]. In PLLC, PCL acts as soft matrix and PLA as hard domains [30]. Electrospun PLLC has been used for various tissue engineering applications such as nerve tissue engineering [31], bone tissue engineering [32], vascular grafts [33], tendon tissue engineering [34], and urinary bladder regeneration [35]. The PLLC matrix-based systems are not yet studied in the area of wound dressings and as a controlled dermal drug delivery platform. On the other hand, collagen is a biopolymer having a most important structural element in native ECMs. Collagen has a triple helical structure with a high glycine content, which improves the attachment and proliferation of cells throughout the matrix, and mimics the function of the native cells [36]. Therefore, collagen-based materials are currently most favored in biomaterial fabrication [37]. Incorporation of collagen in PLLC will enhance bioactive sites in electrospun mats and cause an increased migration and proliferation of new cells at wound sites.

An antibacterial model drug gentamicin was incorporated with the PLLC/collagen electrospun matrix. Gentamicin is widely used antibiotic with low cost, good stability and act against several infection caused by Gram-positive and Gram-negative bacteria. Gentamicin irreversibly hinders the 30S ribosomal subunit of bacteria and causes misreading of bacterial t-RNA molecule. In the presence of gentamicin, the microorganisms are incapable to synthesize essential growth proteins and thus prevent spreading of the infection [38]. Intramuscular injection and oral ingestion of gentamicin was not efficient for preventing wound infections because the drug cannot readily reach infectious sites at avascular tissues. Moreover, high dosages and frequent systemic administration of gentamicin may induce severe side effects such as nephrotoxicity and ototoxicity [39]. Fabrication of an electrospun drug delivery matrix with sustained drug delivery kinetics was an ideal strategy for preventing trance dermal wound infections. Gentamicin-loaded PLLC/collagen nanofiber mats are expected to display sustained release characteristics as functional dressings for wound healing applications. Both hydrophilic and hydrophobic parts present in electrospun fibers impart a high efficiency in drug loading.

The objective of the work is to fabricate PLLC/collagen-layered mats using electrospun technique for wound dressing applications. A detailed characterization in terms of morphology, water-uptake ability, water vapor permeability, mechanical properties, and biocompatibility was performed in both pure PLLC/collagen and drug-incorporated electrospun mats. The sustained drug delivery properties and antibacterial effect of the PLLC/collagen electrospun mats were evaluated with HPLC and agar disc diffusion methods. *In vitro* cell culture studies of 3T3 fibroblasts also performed for analyzing the cell proliferation behavior of the scaffolds.

2. Experimental

2.1. Materials

ε-Caprolactone was purchased from Sigma-Aldrich USA and L-Lactide (98 + %) was obtained from Alfa Aesar. Tin (II) 2-ethylhexanoate (95%) was purchased from Sigma-Aldrich, Japan and completely dried by distillation over calcium hydride (CaH_2). 1,1,1,3,3,3-hexafluro-2-propanol (99%) (HFIP) (Sigma-Aldrich, China), Collagen from bovine achilles tendon (Sigma-Aldrich, USA), gentamicin sulfate (Sigma-Aldrich, China) were purchased. Methanol and chloroform were purchased from Merck India Ltd. Albumin bovine (BSA) was purchased from SRL India. Micro BCA protein assay kit and Mueller-Hinton agar were purchased from Thermo Scientific (USA) and Himedia (India), respectively. 3T3-L1 mouse fibroblast was obtained from National Centre for Cell Sciences Pune (India). Cell culture media, supplements, and the other chemicals were obtained from Sigma-Aldrich (USA). Phosphate-buffered saline (PBS) was prepared according to the literature [40].

2.2. Synthesis of poly(L-lactide-co-ε-caprolactone) copolymer

The PLLC copolymer was synthesized according to the literature [41,42]. An equal amount of L-lactide and ε-caprolactone (0.367 mol) was taken in a two-neck 250-mL round-bottom flask. The catalyst stannous octoate is diluted with dried toluene at a concentration of 1×10^{-4} mol. Toluene was distilled off and copolymerization was performed at 150°C in silicone oil bath for 24 h with stirring. After completion of copolymerization, PLLC was dissolved in chloroform followed by precipitation into an excess amount of methanol, and dried under vacuum at room temperature for 2 days.

2.3. Preparation of PLLC/collagen nanofibers mats

A series of PLLC/collagen solutions with different concentrations were prepared by dissolving them in HFIP with a solution concentration of 15%. The collagen concentrations were varied from 10, 20, and 30 wt%. Spinning was performed at a predetermined condition of 15% solution concentration, 18 kV applied potential, 1 mL h^{-1} feed rate, 12-cm needle tip to collector distance with a 500 rpm rotating mandrel collector. The desired solutions were loaded into a 10-mL syringe, the opening end of which was connected to a 21 gauge

stainless steel needle that was used as the nozzle. High-voltage power supply and syringe pump (Holmark) were used to generate a high-DC potential as well as to control the feed rate of the polymer solution. PLLC/collagen/gentamicin electrospun mats are prepared by inclusion of 10 wt% drug into 80:20 PLLC/collagen blend solution. In layered PLLC+C+G electrospun mat, the middle layer was loaded with 90:10 PLLC/gentamicin and the outer two layers with 80:20 PLLC/collagen. The formulations of samples with sample codes have been given in Table 1. All experiments are performed at room temperature and atmospheric humidity conditions within a fixed collection time of about 7 h and the thickness of the sample obtained was noted. After the process, the electrospun fibers were dried in a vacuum oven at 40°C for about 48 h to remove the residual solvent.

2.4. Chemical analysis

The copolymer and electrospun scaffolds were tested with Fourier transformation infrared spectroscopy (FTIR) by KBr pellet as well as ATR mode on an infrared spectrometer (Nicolet 5700) in 4,000–400 cm^{-1} gel-permeation chromatography (GPC) measurements of the synthesized copolymer (PLLC) were performed using a 0.05% polymer solution in Waters HPLC system, 600 series pump with tetrahydrofuran as the mobile phase with a flow rate 1 mL min^{-1}, and polystyrene standards of molecular weight (100000/34300/3250).

2.5. Scanning electron microscope

The morphological characterization of electrospun fibers were performed by scanning electron microscope (SEM, Hitachi 6600), at an accelerating voltage of 10 kV. The fiber diameters from SEM images were analyzed using the Image J software and the average fiber diameter was calculated from at least 50 fibers.

2.6. Mechanical testing

The mechanical properties of electrospun scaffolds of dimension 0.5 × 5 cm were investigated using a universal testing machine (Schimadzu Autograph, AG-Xplus series) with an applied load of 10 N. For each sample, 5 specimens are tested.

2.7. Water contact angle, water permeability, and sorption

Electrospun mat cut in 1 × 3-cm dimension rectangles and 1-μL water drop was placed. The images of the water drop on the sample surface were captured by a goniometer digital camera and processed by software program (DIGIDROP). Each sample was measured at 15 different locations and the readings were averaged. Water vapor permeability (WVP) studies of electrospun PLLC/collagen mats were performed by a modified ASTM standard test [43]. WVP experiments are performed in a desiccator with constant relative humidity. The circular dimension mats were fixed on the neck of 3 × 5 cm permeation bottles. The weight differences of the bottles with water and electrospun mat were evaluated at different time intervals.

The WVP of a membrane was calculated by the equation:

$$\mathrm{WVP} = \frac{-\Delta \mathrm{W}}{A \times \Delta t} \tag{1}$$

where ΔW is the change in weight of water, A is the exposure area of the electrospun mat, and Δt is the exposure time.

The electrospun mats of dimension 0.5 × 5 cm was initially weighed and immersed in 10 mL of PBS solution at 37°C for different time intervals. Water adsorption (WA) of the electrospun mats were calculated using the following equation.

$$\mathrm{WA} = \frac{W_a/M}{W_i} \times 100 \tag{2}$$

where W_a is weight of electrospun mat after immersing in PBS, M is molecular weight of water, and W_i is the initial weight of electrospun mat.

Table 1. Formulations of samples with sample codes.

Sample code	Sample description
PLLC	PLLC
PLLC+G	PLLC + 10% gentamicin
PLLC+C	PLLC + 20% collagen
PLLC+C+G	PLLC + 20% collagen + 10% gentamicin
PLLC+C+G Layered	PLLC + 20% collagen: outer layers PLLC + 10% gentamicin: inner layers

PLLC, poly(L-lactide-*co*-caprolactone).

2.8. Blood clotting assay

The whole blood clotting assay was performed based on the literature [44]. Blood was mixed well with anticoagulant agent acid citrate dextrose at a ratio of 9:1. Triplicate samples were used for this study and pure PLLC electrospun mat was assigned as a negative control. Blood with 1% anticoagulant was added to 1 cm^2 of PLLC/collagen nanofibers mats placed in 25-mL plastic Petri dishes. Immediately 10 μL of 0.2 M $CaCl_2$ solutions was added to each Petri dish to initiate the blood clotting and incubated for 10 min at 37°C. A quantity of 15 mL of distilled water added dropwise without disturbing the clot. Subsequently, 10 mL of solution was taken from the dishes and was centrifuged with 1,000 rpm for 1 min. The supernatant was collected for each sample and incubated at 37°C for 1 h. The optical density of the supernatant was measured at 530 nm using UV–Vis spectrophotometer.

2.9. Protein adsorption studies

The different electrospun mats with a dimension 1 × 1 cm (triplicates) were immersed in 10 mL of PBS for 24 h at room temperature for equilibration. After that the mats were dipped in a solution containing 4.5 mg mL^{-1} of BSA for 12 h at 37°C and subsequently rinsed thrice with PBS solution. The membranes were subjected to 1-h sonication in 0.5 mL of 1 wt% sodium dodecyl sulfate solution for complete desorption of BSA. The absorbance of different samples and standard solutions was measured with UV–Vis spectroscopy (Perkin Elmer-Lambda 35) at 562 nm.

2.10. In vitro degradation studies of scaffold

Different electrospun mats were cut into rectangular pieces with dimension of 50 × 5 mm for biodegradability tests within a scheduled time (28 days). The electrospun mats were dipped in 10 mL of phosphate buffered solution (PBS, pH = 7.4) and incubated at 37°C for different time periods such as 2, 7, 14, 21, and 28 days. After each incubation period, the samples were withdrawn from the bottle and dried well using vacuum oven. The dried samples were subjected for SEM analysis and mechanical testing to observe the morphological as well as mechanical changes occurred during the period of the degradation process.

2.11. Antibacterial studies and in vitro drug release studies of electrospun scaffolds

The relative antimicrobial activities of gentamicin-incorporated electrospun mats were determined using the disc diffusion method in Mueller–Hinton agar. Samples were cut into 1-cm diameter discs and placed in 5-mL glass bottles (one sample per bottle, total number = 3) containing 1 mL of phosphate buffer solution (0.15 mol, pH 7.4) each. Six microliters of solution were pipetted out after each 24 h of incubation at 37°C and placed on 6-mm discs. The discs were placed on Mueller–Hinton agar plates seeded with a layer of Gram-positive bacteria *Staphylococcus aureus* and Gram-negative bacteria *Escherichia coli.* The zones of inhibition were measured with a Vernier after 16–18 h of incubation at 35°C. The bioactivities of the incubated gentamicin on *S. aureus* and *E. coli* were determined by:

$$\text{Bioactivity}\,(\%) = \frac{\text{Diameter of sample inhibition zone}}{\text{Diameter of maximum inhibition zone}} \quad (3)$$

In vitro release behavior of residual gentamicin from the PLLC/collagen electrospun mats were evaluated by antibacterial assay. All the electrospun mats were cut into 1 × 1-cm^2 pieces and placed over previously wetted agar plates with 1 mL of sterilized water, to evaluate the time course of the drug release. The electrospun mat was removed from the wet agar surface and immersed into 1 mL of distilled water and shaken continuously for 2 days to leach out the whole amount of gentamicin. The gentamicin percent in the leach out solution was quantitatively analyzed by HPLC (Shimadzu-Prominance) as per the literature [45]. From the initial and residual amount of gentamicin measurements, the release percentage of gentamicin was calculated. Drug release quantification was performed five times for each electrospun mat and the average was taken. Gentamicin release profiles on wet agar plates from the nanofibrous mats were also evaluated using the inhibition of *E. coli* after different time intervals of treatment. At different time intervals, electrospun mats were removed from the wet agar plates and placed upon a new agar plate containing *E. coli* for further evaluation of inhibitory effect from the residual gentamicin. Finally, the agar plates were incubated at 37°C for 16 h and the inhibition zones were measured by Image J software. For each sample, the above experiment was performed in triplicate.

2.12. Cell proliferation assay

The 3T3-L1 mouse fibroblast cells were cultured in Dulbecco's modified Eagle's medium containing 10% fetal bovine serum, 1.2% pen strep, and 0.2% amphotericin B in an atmosphere of 5% CO_2 at 37°C. Cell proliferation was measured by the MTT assay. Sterile electrospun mat of PLLC/collagen of around 600-μm thickness was cut into small squares (1 × 1 cm) and soaked with cell culture medium. 2×10^5 cells mL^{-1} were seeded on the scaffold. Minimum of triplicate of test samples will be seeded. Cell-seeded scaffolds were incubated at 37°C in humidified atmosphere with 5% CO_2 for 4 h to make cells diffuse into and adhere to the scaffold and later on 250 μL of culture media is added into each well. A quantity of 30 μL of 5 mg mL^{-1} tetrazolium dye MTT (3-(4,5-dimethylthiazol-2-yl)-2,5-diphenyltetrazolium bromide) was added to each well after 1st, 3rd, and 5th day of incubation and were incubated at 37°C in humidified atmosphere with 5% CO_2 for 2 h and the absorbance was read at 590 nm with a reference filter of 620 nm using Synergy HTMulti-Mode Microplate Reader (BioTek).

2.13. Statistical analysis

All the experiments were conducted in triplicate. The results are presented as the mean and S.D. analysis of variance and a student's *t*-test were performed to determine the significant differences among the groups. Statistical analysis was performed with the SPSS 22 Software Program (SPSS Inc., USA). Differences were considered significant for $p < 0.05$.

3. Results and discussion

3.1. Characterization of PLLC

Poly(L-lactide-*co*-caprolactone) random copolymer was synthesized by ring-opening polymerization of L-lactide and ε-caprolactone in the presence of stannous octoate [$Sn(Oct)_2$] in bulk at 150°C. The yield of PLLC copolymer was around 55%. The number average molecular weight (Mn) and polydispersity (Mw/Mn) of the PLLC copolymer determined by GPC were 65000 and 3.7, respectively.

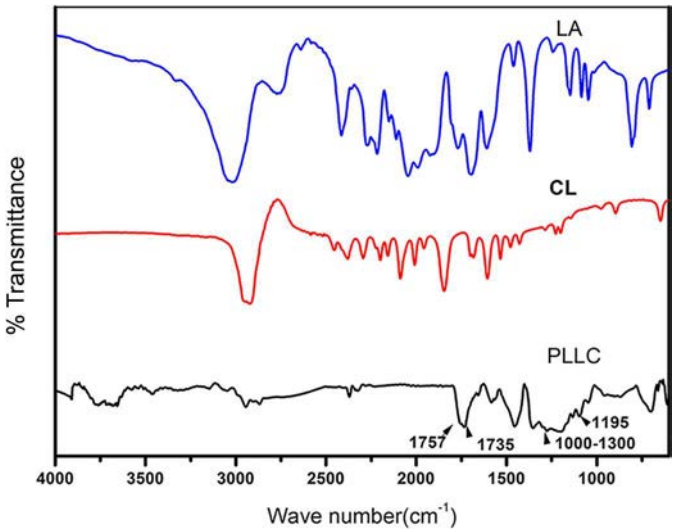

Figure 1. FTIR spectra of LA, PCL, and PLLC copolymer.

Figure 1 shows FTIR peaks of L-Lactide, ε-caprolactone, and PLLC copolymer. The PLLC copolymer exhibits two carbonyl stretching peaks at 1,734 and 1,757 cm^{-1} because of the C=O group present in PCL and PLA, respectively. A peak splitting was observed in the above range is due to the presence of an equal amount of both the monomers. The peaks around 1,300–1,000 cm^{-1} is due to the presence of the ester group, and peak at 1,195 cm^{-1} indicates the ester group of long chain alkynes. These peaks confirm that the final product obtained is PLLC random copolymer. Bands at 2,997 cm^{-1} of PLA, 2,946 and 2,862 cm^{-1} of both PLA and PCL are present due to stretching of alkyl groups in copolymers of PLLC. The absence of band at 2,997 cm^{-1} in PCL is in agreement with the statement that CH stretching at 2,990 cm^{-1} was characteristic of PLA component present in PLLC copolymers.

3.2. Morphology of electrospun PLLC/collagen fibers

Morphology of PLLC and PLLC/collagen blend nanofibrous mat at different concentrations have been illustrated in Figure 2. All the images show randomly oriented fibers with a cylindrical smooth fibrous morphology in nanometer range of diameters without any bead formation. The pristine PLLC electrospun fibers exhibit an average fiber diameter range of 382 ± 93 nm. The electrospun mats with 10 and 20 wt% collagen showed average fiber diameters of 178 ± 60 and 141 ± 35 nm, respectively. The average fiber diameter of PLLC/collagen nanofibrous mat decreased with the increase in collagen concentration. In electrospinning, the fiber formation has been occurred by stretching of solution jet due to the repulsive forces in between the charged solution. Collagen is an amphiprotic macromolecule, which consists of large side-chain amino acids and hydrophilic blocks as well as charged amino acids. The higher collagen concentration induces an increase in charged ion density in electrospun solution, which induces excess elongation force on tailorcon results to yield a smaller fiber. From an optimum concentration 80:20 PLLC/collagen, further addition of collagen in 70:30 ratio causes a slight increase in fiber diameter to 293 ± 64 nm. This phenomenon is due to incomplete miscibility between PLLC and collagen, thus for 70:30 PLLC/collagen concentration the fiber diameter slightly increases. The nanofibrous mat with minimum fiber diameter was considered as an ideal material for tissue engineering applications. The nanofibrous mats with minimum fiber diameter will offer large surface area to volume ratio for tissue regeneration, migration, and proliferation as a scaffold, moreover exhibited excellent drug release behaviors. Thus, electrospun nanofibrous mat with 20 wt% of collagen (PLLC+C) having minimum fiber diameter is used for further analysis.

Figure 2e–f shows the morphology of drug-incorporated electrospun mats. Two strategies were adopted for fabrication of drug-incorporated PLLC/collagen nanofibers mats. The former includes simple blending of 10% of gentamicin with PLLC/collagen (80:20) matrix (PLLC+C+G). Gentamicin is a type of aminoglycoside. As a result, loading of gentamicin in PLLC/collagen matrix leads to an increase in fiber diameters to 276 ± 50 nm. The second method involves the formation of layered electrospun nanofibrous mats having a sandwich-like structure, in which the middle layer was incorporated with drug and PLLC. The two outer layers were prepared by spinning of PLLC/collagen (PLLC+C+G Layered). Figure 2f clearly helps to distinguish beween the existing drug-incorporated inner layer and thin PLLC/collagen nanofibrous outer layer. A schematic of drug-incorparated layered electrospun mats has been given in Figure 3.

3.3. Mechanical properties of electrospun nanofibrous mats

An ideal wound dressing material should have sufficient mechanical strength for proper handling and should be in

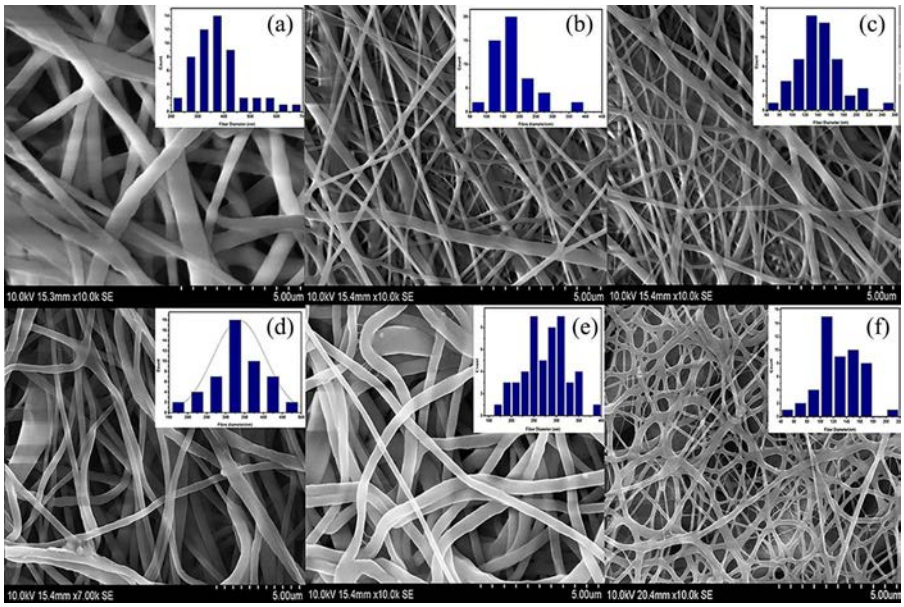

Figure 2. SEM images of electrospun PLLC/collagen with a concentration of (a) PLLC, (b) PLLC/collagen (90:10), (c) PLLC/collagen (80:20), (d) PLLC/collagen (70:30), (e) 10 wt% gentamicin loaded PLLC/collagen, and (f) 10 wt% gentamicin loaded layered PLLC/collagen nanofibers.

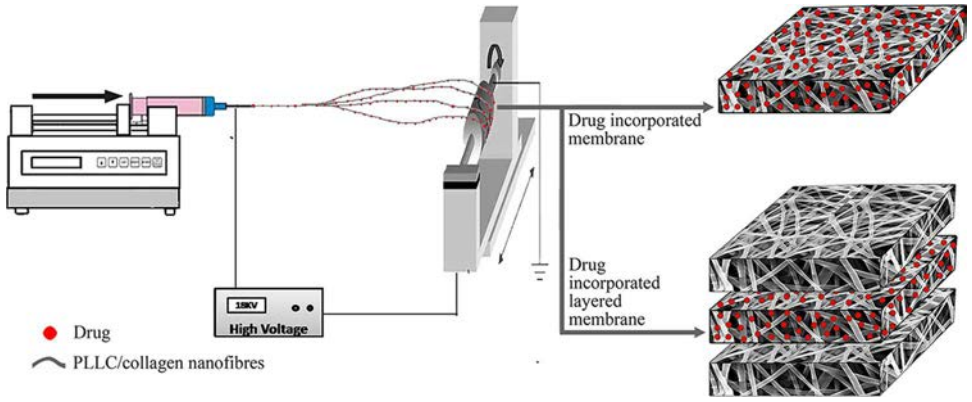

Figure 3. Schematic reprecentation of drug incorparated layered membrane.

proper sterilized condition before applying on the wound surface. The tensile properties and percentage of elongation of electrospun PLLC/collagen nanofibers mats were characterized and are summarized in Table 2. The PLLC electrospun mats showed a very soft and flexible characteristic with high elongation at break of 944% and tensile strength of 8.13 ± 0.41 MPa. Inclusion of 20% collagen in PLLC induce an increased elongation at break to 1,633% and tensile strength 12.01 ± 0.98 MPa, due to long-chain entangled triple-helical structure of collagen and high compatibility between PLLC and collagen. The tensile strength at break exhibited a noticeable behavior in the case of gentamicin-loaded PLLC/collagen nanofibers. By the addition of 10% gentamicin in PLLC (PLLC+G), the tensile strength increased by 9.7% but in the case of PLLC/collagen drug incorporation (PLLC+C+G) induces a drastic increase of 57.6% in tensile strength. It would be due to the high uniform miscibility of gentamicin with the PLLC/collagen and it is also acting as reinforceable filler content in the matrix. But the drug content will increase the brittleness of the electrospun mats, and elongation at break has been reduced to 227% for PLLC+G and 464% for PLLC+C+G. PLLC+C+G-layered electrospun mats exhibit an increase in tensile strength of 19.8 ± 0.638 MPa. In any case, such an enhanced strength and elongation of PLLC+C+G electrospun mats would be very beneficial for use in skin tissue engineering scaffolds and as a wound dressing material.

3.4. Water contact angle

Excessive production of wound extrudates is a common problem faced in the early stages of wound healing. The ideal wound dressing should have the ability to absorb extrudates and infectious components, which makes the wound chronic by microbial infection. Water contact angle measurements illustrate fluid interaction behavior of electrospun nanofibrous mats. Figure 4a demonstrates contact angle variation of different PLLC/collagen fiber mats. The pristine PLLC electrospun mats showed a slight hydrophobic nature with a contact angle of around $121.5 \pm 1.3°$. Inclusion of 20 wt% natural macromolecular protein collagen in PLLC improves the hydrophilicity of scaffold to $86.62 \pm 1.23°$. The lower contact angle indicates higher hydrophilicity. The optimal contact angle values for protein adsorption and cell adhesion are of 40–85° [46]. Furthermore, the hydrophilicity decreases markedly to $112.71 \pm 0.83°$ with the addition of gentamicin also. This decrease is mainly due to the noncovalent hydrogen-bonding interaction generated between the terminal hydroxyl and amino groups on the collagen chains and gentamicin. For PLLC+C+G- and PLLC+C+G-layered scaffolds, the contact angles observed were $85.14 \pm 3.21°$ and $85.86 \pm 0.59°$, respectively. As per the above results, PLLC+C+G-layered samples showed better hydrophilicity and can be considered as a good candidate for wound dressing.

Table 2. Tensile strength, elongation at break of PLLC/collagen scaffolds.

Sample	Tensile strength (MPa)	Elongation at break (%)
PLLC	8.13 ± 0.41	944 ± 50
PLLC+G	8.92 ± 0.53	227 ± 48
PLLC+C	12.01 ± 0.98	1633 ± 74
PLLC+C+G	18.92 ± 1.4	464 ± 63
PLLC+C+G Layered	19.86 ± 0.63	560 ± 47

PLLC, poly(L-lactide-*co*-caprolactone).

3.5. Water vapor permeation and sorption studies

Wound dressing materials should provide sufficient permeability toward water vapor to attain rapid wound healing as well as to prevent secondary infections. If the wound dressing material does not have sufficient water vapor permeation capacity, the wound become dehydrated and in some cases excess wound-extrudate formation becomes a major cause of infections. Figure 4b illustrates the WVP of different PLLC/collagen scaffold. The decrease in WVP in PLLC electrospun mats ($1{,}562 \pm 12$ g m^{-2} per day) is due to comparatively high hydrophobicity and its poor absorption of water vapor, resulting low transfer across the mat. Fiber diameters of electrospun mats also have a role in water vapor permeation capacity. Smaller-diameter electrospun mats resulted in an increase in pore density and subsequently show better wicking and vapor transmission rate. WVP of normal skin is about 204 g m^{-2} per day and that for injured skin is in a range from 279 g m^{-2} per day, for a first degree burn it will be around 5,138 g m^{-2} per day for granulating wound. To prevent the risk of wound dehydration the recommended WVP should be in the range of 2,000–2,500 g m^{-2} per day [47]. By

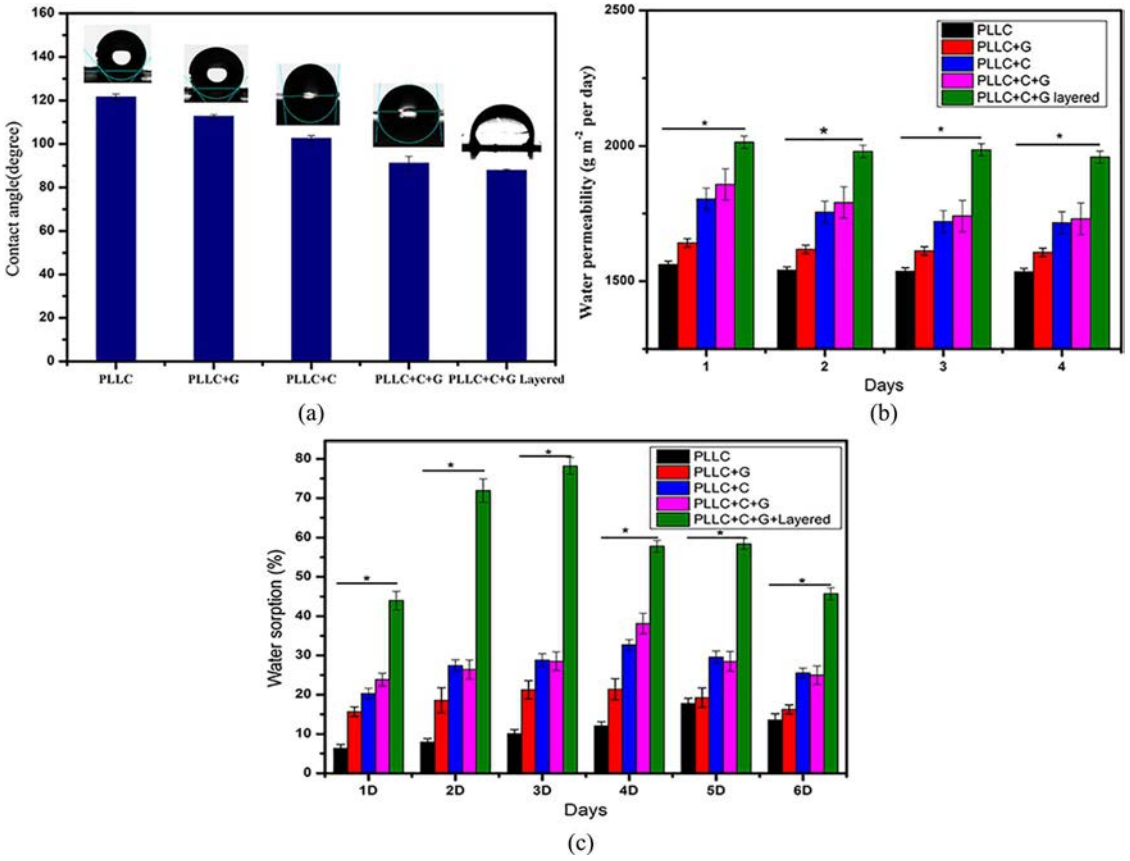

Figure 4. (a) Water contact angles of PLLC/collagen electrospun membranes, (b) water vapor permeability of PLLC/collagen electrospun membranes at different time intervals, and (c) water adsorption capability of PLLC/collagen electrospun membranes with different time intervals (* indicates a statistical difference [$p < 0.05$] between the pair).

incorporation of hydrophilic components collagen and gentamicin, the WVP increased to $1{,}858 \pm 85\ g\ m^{-2}$ per day. The increase in WVP in PLLC+C+G electrospun mat is also due to the decrease in fiber diameter. PLLC+C+G layered electrospun mat also showed a higher WVP of $2{,}014 \pm 22\ g\ m^{-2}$ per day. The above results elaborate a positive indication for the PLLC+C+G electrospun mat being used in wound dressing.

Accumulation of wound extrudates in wound site is a major problem faced in the early stages of wound healing, which is a serious cause of infection in the wound site. Quick sorption of extrudates from wound surface will lead to quick healing of the necrotic tissues and facilitates the re-epithelialization. Figure 4c reveals water sorption percentage of different PLLC/collagen electrospun mats at different time intervals. However, it can be seen from the figure that the pure PLLC electrospun mat shows the lowest water uptake during a 24 h test period because of its comparably high hydrophobic nature. Meanwhile, PLLC+C, PLLC+G, PLLC+C+G electrospun mat exhibit higher water sorption percentage, which implies that the mat becomes hydrophilic with the incorporation of the collagen and gentamicin. The inclusion of gentamicin and collagen in PLLC causes an increase in swelling behavior and water sorption capacity due to the minimum fiber diameter, high pore density and hydrophilicity of the foreign components included. In the case of collagen-incorporated electrospun mat, the slight weight loss occurs from day 4, because of the degradation of hydrophilic long-chain collagen strand. Water sorption percentage of PLLC+C+G-layered electrospun mat is maximum due to the hydrophilicity of the outer PLLC and collagen layer. Such desirable properties will be beneficial for the wound healing.

3.6. In vitro *degradation studies*

Biodegradability is an important parameter for the selection of materials in the field of tissue engineering and wound dressing. Thus, an *in vitro* degradation study in PBS at 37°C was conducted and evaluated with morphological analysis and mechanical testing. Figure 5a–e shows the SEM micrographs of different scaffolds during the degradation process after 28 days. The rate of degradation is affected by several parameters such as molecular weight, hydrophilicity, the degree of crystallinity, and level of porosity. All the five scaffolds are partially degraded within 28 days, but the fiber morphology can be clearly observed. First-step polymer electrospun mat degradation starts from swelling of individual fibers. Figure 5f illustrates the fiber swelling in different days of degradation. All the scaffolds are swollen on the 14th day and collagen-incorporated PLLC scaffold shows increased fiber swelling behavior compared to others. The presence of hydrophilic collagen allows a fast influx of water molecules and build-up of osmotic pressure within the matrix. The pure PLLC and PLLC+G scaffold showed only 25% fiber diameter elevation due to swelling. However, the collagen inclusion in

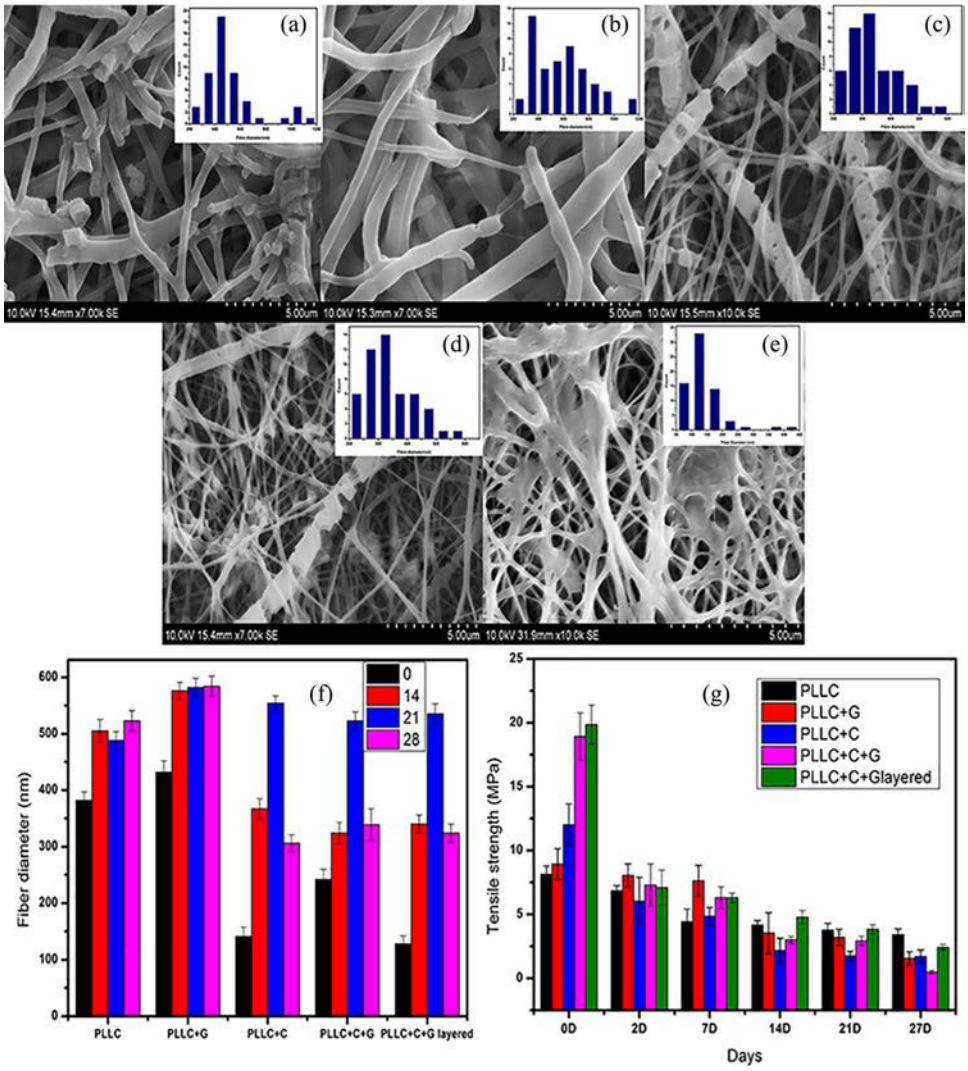

Figure 5. SEM images of (a) PLLC, (b) PLLC+G, (c) PLLC+C, (d) PLLC+C+G, and (e) PLLC+C+G layered fibers after 28 days of PBS degradation. (f) Average fiber diameter of scaffolds with different days of degradation. (g) Mechanical studies of scaffolds after different days of degradation.

polymer matrix (PLLC+C) considerably increased the swelling up to 61% due to the acceleration in hydrophility. Even though the addition of drug gentamicin does not show much effect on fiber swelling, the role played by them in electrospun mat due to its high-water solubility nature is significantly important. In the case of collagen-incorporated scaffolds, the fiber diameter decreased from 21st day, which means the second stage of degradation was started from 21st day onward. On 28th day, the nanofiber strands visibly started breaking.

Evaluation of degradation in PLLC/collagen electrospun mats are also done by mechanical studies. Figure 5g reveals the tensile strengths of electrospun nanofibers with different days of degradation. The tensile strength results reveal a drastic change in strength from the second day onward. The high pore density and surface areas-to-volume ratio of electrospun mat accelerated the degradation rates. Neat PLLC shows a decrease in tensile strength about 58% after 28 days, ascribed to hydrolytic degradation of aliphatic ester linkages that begin with a water-uptake phase followed by random hydrolytic cleavage of the ester bonds. From the tensile strength results, it is confirmed that collagen incorporation accelerated the PLLC fiber degradation. PLLC and PLLC+G nanofiber mats showed 58% as well as 82% decrease in tensile strength within 28 days. But collagen-incorporated PLLC+C-, PLLC+C+G-, and PLLC+C+G-layered samples show tensile strengths of 85%, 97%, and 87%, respectively. So PLLC+C+G- and PLLC+C+G-layered samples undergo major degradation within 28 days. For chronic wound, the complete reconstruction of the epithelial layer will take 2–3 weeks, so it can be used as a good candidate for biodegradable drug-loaded wound dressing material.

3.7. Protein adsorption and whole blood clotting assay

The nonspecific protein adsorption is a major concern in the performance of tissue engineering scaffolds in the biomedical field. The amount of BSA adsorbed per unit surface area on the electrospun PLLC/collagen electrospun mat at 37°C is given in Figure 6a. The pristine PLLC electrospun mat was taken as negative control and a blank reagent solution without any sample is taken as positive control. PLLC electrospun mat exhibited BSA $1.70 \pm 0.20\,\mathrm{kg\,m^{-2}}$ adsorption. Adsorbed BSA per unit surface area of the various PLLC/collagen electrospun scaffolds were decreased from 1.54 ± 0.33 to $0.491 \pm 0.02\,\mathrm{kg\,m^{-2}}$.

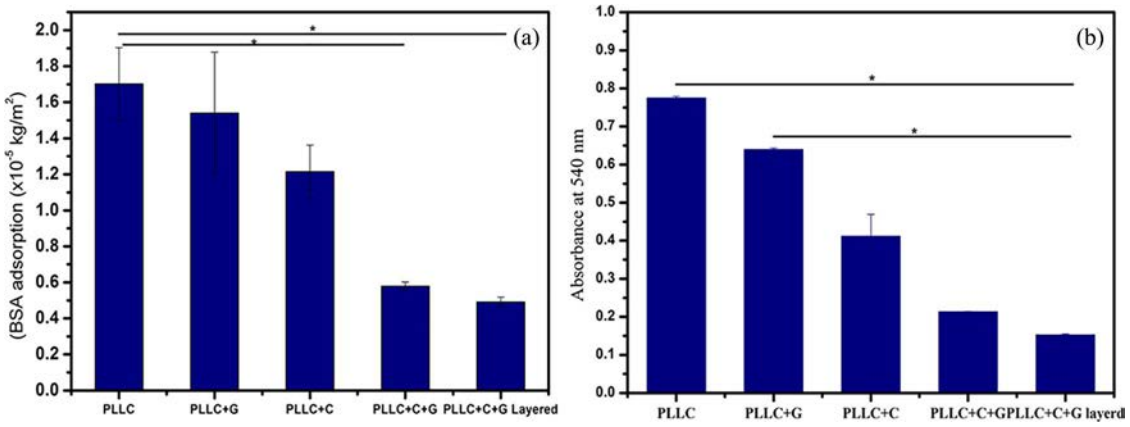

Figure 6. (a) Protein adsorption in different electrospun scaffolds and (b) blood clotting assay of different electrospun scaffolds. (* indicates a statistical difference [$p < 0.05$] between the pair).

The protein adsorption is due to the hydrophobic interaction between the substrate and the protein. Membranes with low hydrophilic character can absorb larger amount of protein. This decrease in BSA adsorption is due to the effect of hydrophilic components such as collagen and gentamicin on the electrospun mat surface which makes it less interactive with the protein. To attain biocompatibility and to accelerate cell proliferation, the electrospun mat should adsorb minimum quantity of protein on its surface. The PLLC+C+G and PLLC+C+G layered samples exhibited 66% and 71% of the decrease in BSA adsorption compared to the pure PLLC scaffold.

For trance dermal wound dressing system hemostatic potential is a significant property to prevent excess bleeding and facilitates hemostasis in early stages of wound healing. The hemostatic potential was evaluated by conducting whole blood clotting assay. The absorbance values of the resultant hemoglobin solution after blood clot were measured at 540 nm and exhibited in Figure 6b. The pristine PLLC is taken as negative control [44]. Inclusion of collagen and gentamicin play a vital role in blood clotting ability of electrospun mats. Only a slight increase in blood clotting ability was occurred by addition of the antibacterial drug gentamicin [48]. But the inclusion of 10% collagen highly facilitates the clotting ability. This is due to the negatively charged phospholipids such as phosphatidylserine present in collagen interact with the platelets surface and form the catalytic surface for the assembly of active coagulation complexes and thrombin generation [49]. As a result PLLC+C+G- and PLLC+C+G-layered electrospun mats exhibited high blood clotting ability and minimizes the excess bleeding at the early stages of wound healing and made them good candidates for wound dressings.

3.8. Antibacterial and drug release studies

The antibacterial activity of the gentamicin-incorporated PLLC/collagen electrospun mat was tested toward Gram-negative *E. coli* and Gram-positive *S. aureus* (Figure 7). The pure PLLC and PLLC+C electrospun mats were evaluated for antibacterial properties, as expected no significant effect was detected. This indicated that these electrospun mats were not capable of any antibacterial effects. Incorporation of gentamicin in PLLC and PLLC+C electrospun mats exhibited excellent antibacterial behavior against both the *E. coli* and *S. aureus*, showing clear zones around the discs. However Napavichayanun et al. was observed the drug and protein incorporation sequence will affect the antibacterial activity [50]. But in the case of PLLC+C+G electrospun mat, the drug and collagen incorporation sequence was independent of antibacterial property. The release characteristics of gentamicin, from the nanofibrous mats were studied using antibacterial disk diffusion method. Figure 8a and 8b illustrates the bioactivity of PLLC+G-, PLLC+C+G-, and PLLC+C+G-layered fibers against *E. coli* and *S. aureus* at different days. The activities of the antibiotics remained high after the electrospinning process also [40]. From Figure 8a and 8b, it is confirmed that

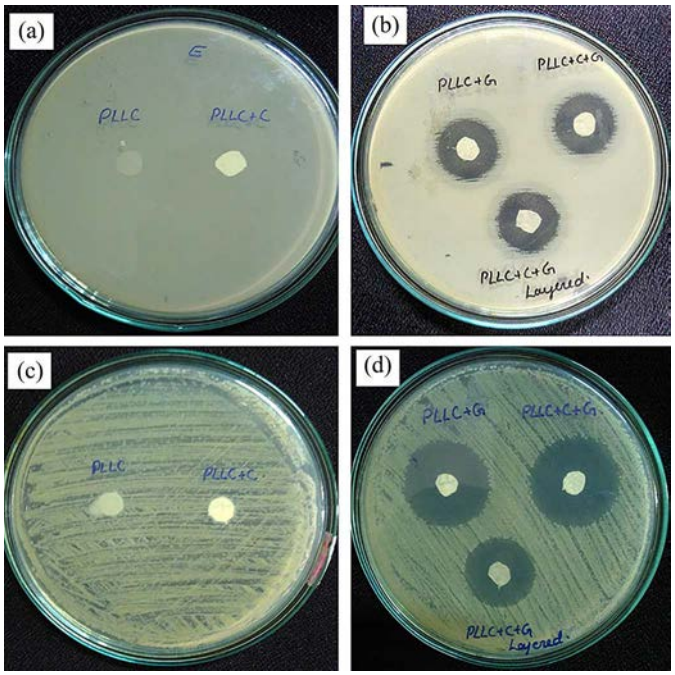

Figure 7. Bactericidal activity of PLLC and PLLC+C against (a) Gram-negative (*E. coli*), (c) Gram-positive (*S. aureus*) as well as bacterial activity of PLLC+G, PLLC+C+G, and PLLC+C+G layered against (b) Gram-negative (*E. coli*) and (d) Gram-positive (*S. aureus*).

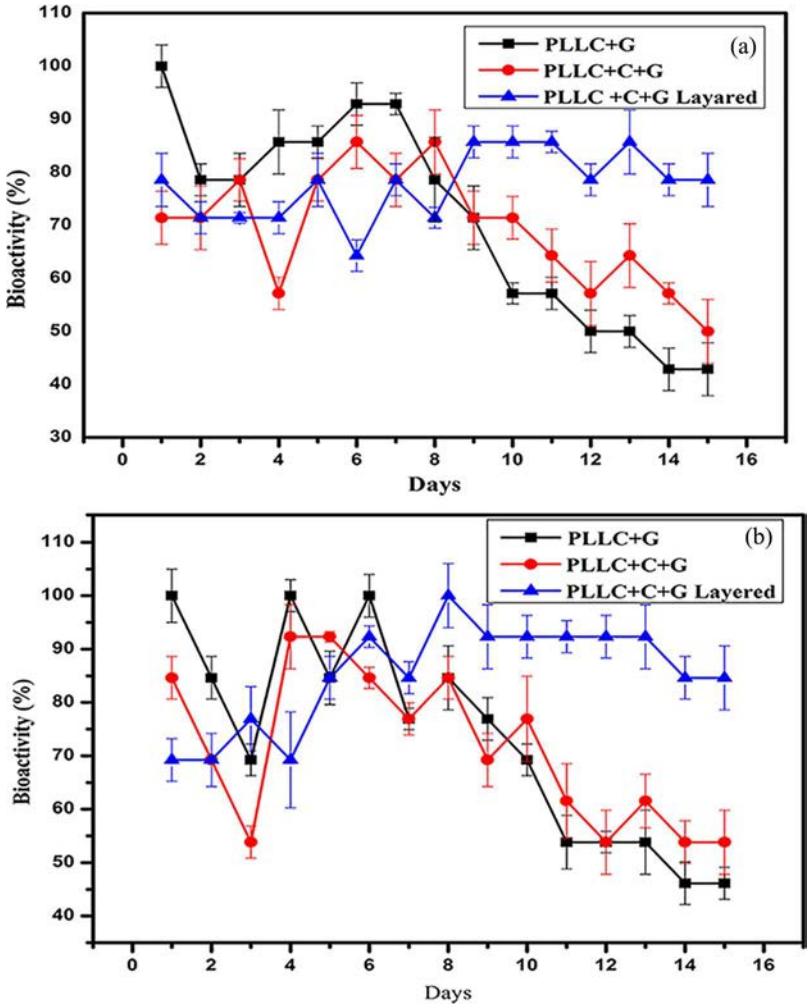

Figure 8. (a) Bioactivity (*E. coli*) of released gentamicin from nanofibers membranes and (b) bioactivity (Staphylococcus) of released gentamicin from nanofiber membranes.

PLLC/collagen nanofibrous mat could maintain the long-term antibacterial effects of gentamicin due to the slow release rate and sustained release profile. In the case of PLLC+G and PLLC+C+G electrospun mat, the bioactivity percentage is high for first few days compared to PLLC+C+G layered electrospun mat, this is due to the initial burst release of gentamicin. PLLC+C+G layered electrospun mat had drug incorporated layer at the center which is covered by two PLLC/collagen layers at both sides, as a result it exhibited bioactivity for 15 days. PLLC+G and PLLC+C+G fibers exhibit a decrease in bioactivity from 10th day while PLLC+C+G layered fibers shows a constant bioactivity rates.

The bioactivity of gentamicin in the liquid medium does not resemble the actual wound environment. It will be desirable if we can achieve the drug release environment similar to the wound surface and study approximately close drug release behavior in that environment. Commonly wounds are wet solid environments with a large amount of extrudates. To duplicate the same condition in the laboratory, the gentamicin release studies were performed by placing the electrospun mat on a prewetted agar plates. In the case of PLLC+G nanofibrous mats, the drug release onto the wet surface was generally fast this was due to the swelling of PLLC nanofibers and high water solubility of gentamicin. In the case of PLLC+C+G and PLLC+C+G layered nanofibers mats, considerably different release patterns were observed. The release profiles were illustrated in Figure 9a. In the case of the PLLC+G electrospun mats the major quantity of gentamicin was released within the first hour. So there is no drastic difference in drug release for following time intervals. PLLC+C+G electrospun mats recovered 5% of the gentamicin after 5 h of application, while those with PLLC+C+G-layered electrospun mat retained 5% drug even after 8 h. But almost complete drug release has occurred within 48 h for all the three PLLC+G, PLLC+C+G, and PLLC+C+G layered nanofibrous mats.

The antibacterial activity of residual gentamicin after the release in the wet solid surface at different time intervals was also evaluated by analyzing the inhibition zones onto the fresh bacterial culture. Figure 9b depicts the area of inhibition of *E. coli* due to residual gentamicin release from PLLC/collagen nanofibers mats. All PLLC+G-, PLLC+C+G-, and PLLC+C+G-layered electrospun mats, the amount of residual gentamicin present is sufficient to exhibit bacterial inhibition zones till 5th hour. After 5th hour, no inhibition zone was observed due to residual gentamicin around PLLC+G electrospun mat

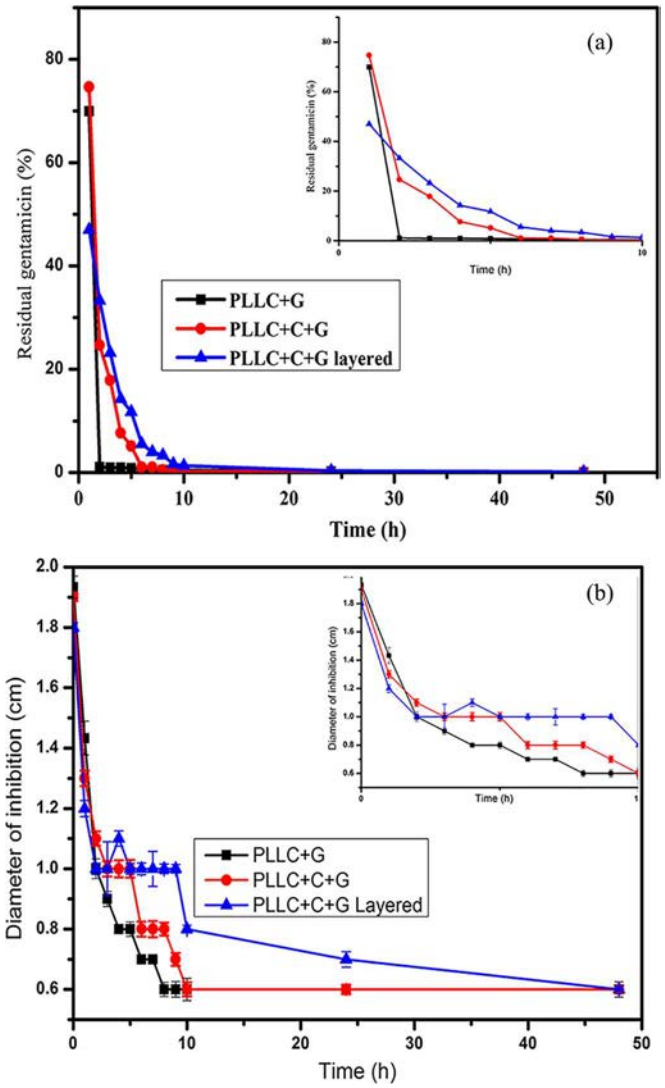

Figure 9. (a) Release profile of gentamicin to agar from PLLC/collagen nanofibers membranes (HPLC), expressed as percentage of residual gentamicin remaining in nanofibers discs and (b) inhibition zones from the residual gentamicin in electrospun membranes after various intervals of gentamicin release in solid agar plates.

due to the complete release of gentamicin. Gentamicin has a particular limiting inhibitory concentration below that the drug release is therefore not detectable in the most distant areas around the nanofibrous mats. PLLC+C+G electrospun mats show inhibitory effect on residual gentamicin for 9 h. Long-chain entangled collagen can trap the gentamicin molecules and cause a slow release of gentamicin in PLLC+C+G electrospun mat. However, prolonged drug release was found for PLLC+C+G layered electrospun mats till 24 h. The drug-incorporated layer in PLLC+C+G-layered electrospun mat was placed as a sandwich-like structure in between two PLLC/collagen electrospun layers. The gentamicin molecule must travel a longer distance from the fiber surface to the free volume.

3.9. Cell growth on electrospun fibrous scaffolds

An ideal wound dressing should be biocompatible, and it should not release any toxic products or produce adverse reactions [51]. Cell viability, morphology, adhesion, and interaction of 3T3 mouse fibroblasts with PLLC/collagen electrospun mats were analyzed by MTT assay and SEM micrographs at 1st, 3rd, and 5th days. The high absorbance value illustrates the viability of 3T3 fibroblast cells. The cell culture plate was used as a control, and the results are summarized in Figure 10. Since the inclusion of collagen and gentamicin did not compromise the biocompatibility of the PLLC nanofibers all the PLLC/collagen electrospun mats exhibited an excellent growth pattern for 3T3 fibroblasts. The cell viability was gradually increasing from the first day to the sixth day for all the electrospun mats. While comparing the different PLLC/collagen samples, dramatic increase in cell proliferation happens for PLLC+C+G- and PLLC+C+G-layered electrospun mats due to its high hydrophilicity and lower fiber diameters. PLLC mat showed comparatively lower cell proliferation patterns compared to other samples, but higher than that of control, which may be due to the shrinkage and hydrophobic surface of the electrospun mat. In the case of electrospun nanofibers mats the cell migration and

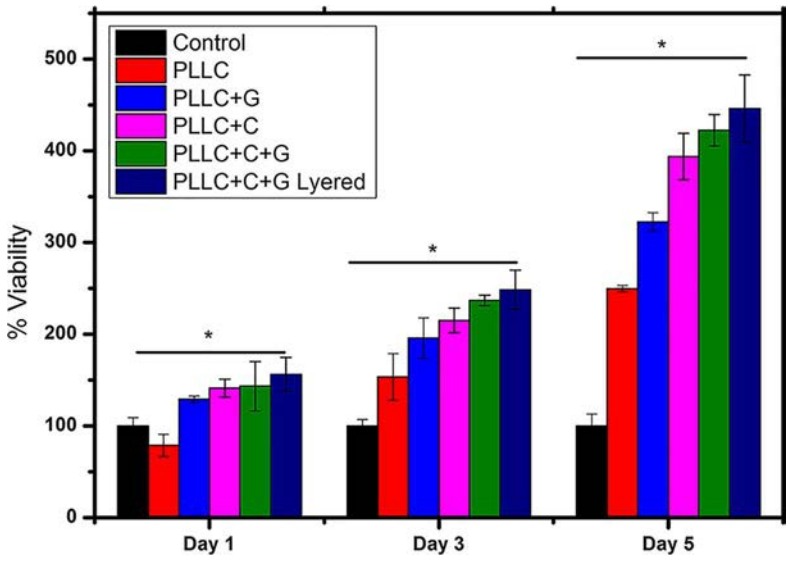

Figure 10. MTT assay of scaffolds using 3T3 fibroblasts at different days (* indicates a statistical difference [$p < 0.05$] between the pair).

proliferation was highly influenced by the pore size, porosity, hydrophilicity, and shrinking behavior. As indicated in Figure 10, the number of viable cells in all nanofibers mats increased drastically during the culture to 5 days. The obtained results clearly suggest that PLLC+C+G- and PLLC+C+G-layered electrospun mats provided highly favorable environments for cell attachment and proliferation and can be suggested as a good candidate to be used for wound dressing.

The morphology of adhered 3T3 fibroblast cells at different days were analyzed by SEM micrographs in Figure 11. It could be found that 3T3 cells appeared to adhere well and exhibited a normal elongated morphology on the electrospun fiber surface, which was due to the large surface area and the availability of interconnecting pores. On 5th day, the cells were overcrowded on the surface of PLLC/collagen, and they were spread with a characteristic spindle-like elongated morphology, which was a clear indication of biocompatibility [52]. The surface wettability and hydrophilicity of electrospun mats have a very strong influence on cell attachment, proliferation, migration, and viability. Pure PLLC nanofibrous matrices do not provide an excellent environment due to its low hydrophilicity and larger fiber diameter. The hydrophilicity of pure PLLC electrospun mat is increased after collagen and gentamicin incorporation. Increased hydrophilicity of PLLC+C+G- and PLLC+C+G-layered electrospun mat showed better cell attachment and more spread morphology.

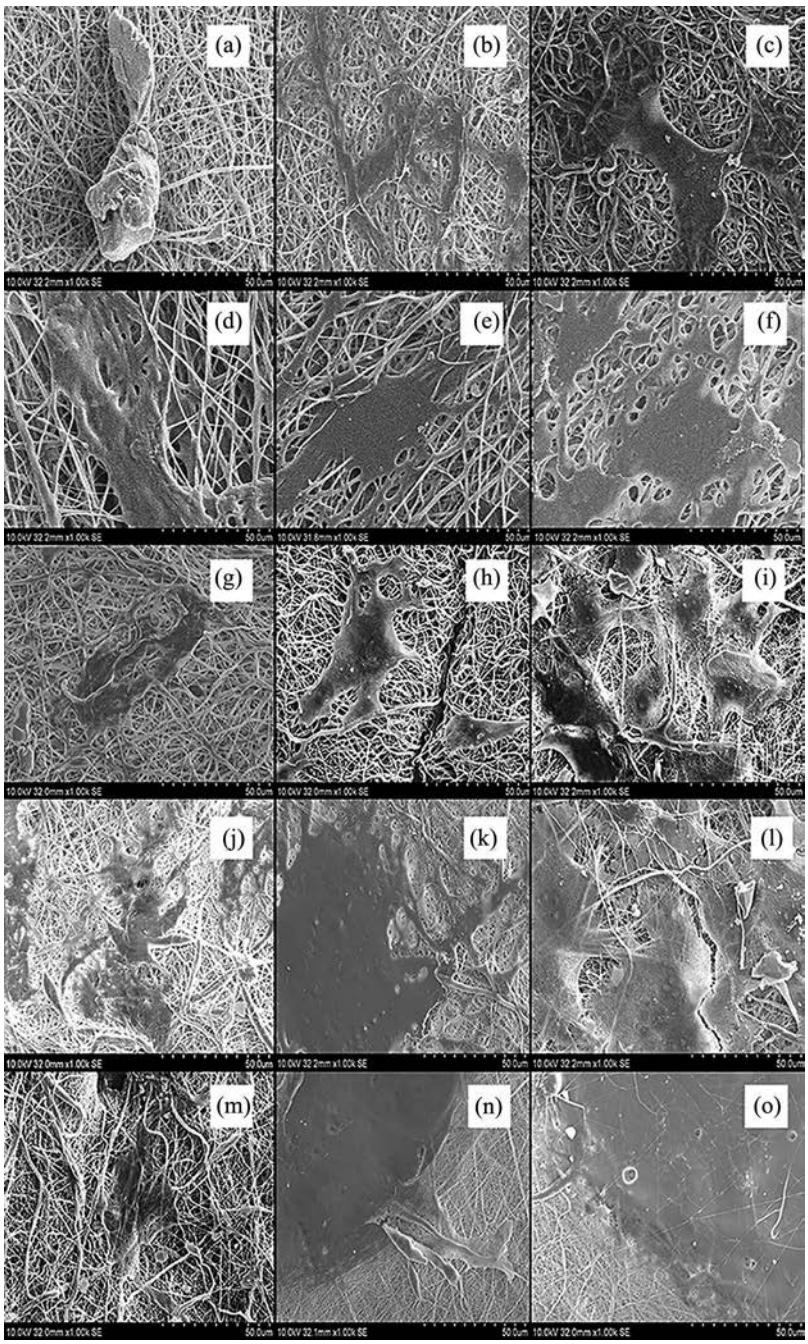

Figure 11. SEM images of 3T3 fibtoblast on PLLC/collagen fibers at different days. First, second, and third day of proliferation of (a–c) PLLC, (d–f) PLLC+G, (g–i) PLLC+C, (j–l) PLLC+C+G, and (m–o) PLLC+C+G layered membranes.

4. Conclusion

This study reports the fabrication of PLLC/collagen electrospun mats as a potential wound dressing and controlled drug delivery membrane. The inclusion of 10% antibacterial drug gentamicin in PLLC/collagen matrix also affects the physicochemical behavior and membrane properties. All the electrospun mats exhibit sufficient flexibility and strength enough to be handled during wound coverage and removal also able to protect from external physical damage. Incorporation of collagen and gentamicin promotes the hydrophilicity, water adsorption and vapor permeation of electrospun mats. PLLC+C+G- and PLLC+C+G-layered electrospun mats exhibit enhanced *in vitro* degradation, blood clotting properties, and reduced protein adsorption. The PLLC+G-, PLLC+C+G-, and PLLC+C+G-layered fibers showed prominent inhibition zones against both Gram-positive bacteria *E. coli* and Gram-negative bacteria *S. aureus*. Compared with other samples PLLC+C+G-layered fibers have a sustained drug release profile and antibacterial effect both in solid and liquid media. The *in vitro* 3T3 fibroblast culture studies exhibited an excellent improvement on cell adhesion and proliferation for PLLC+C+G- and PLLC+C+G-layered fibers due to its high hydrophilicity and surface area-to-volume ratio. PLLC+C+G-layered electrospun mats are promising dressing systems having unique properties such as excellent biocompatibility, proven antibacterial and antioxidant effect, and sustained release profile of the drug. Thereby, they proved their ability to be used for preventing infections and promoting skin regeneration on wound sites. Based on these findings, PLLC+C+G-layered nanofibrous mat can be proposed as an excellent biomaterial for skin wound treatment in the future.

References

[1] Trott, A. T. *Wounds and Lacerations, Emergency Care and Closure*; Elsevier, New York, 2005, pp. 1–336.
[2] Thakur, R. A.; Florek, C. A.; Kohn, J.; Michniak, B. B. *Int. J. Pharm.* **2008**, *364*, 87.
[3] Shevchenko, R. V.; James, S. L.; James, S. E. J. R. *Soc. Interface* **2010**, *7*, 229.
[4] Ovington, L. G. Advances in wound dressings. *Clin. Dermatol.* **2007**, *25*, 33–38.
[5] Jayakumar, R.; Prabaharan, M.; Sudheesh Kumar, P. T.; Nair, S. V.; Tamura, H. *Biotechnol. Adv.* **2011**, *29*, 322.
[6] Tsao, C. T.; Chang, C. H.; Lin, Y. Y.; Wu, M. F.; Wanga, J. L.; Younga, T. H.; Hane, J. L.; Hsiehb, K. H. *Carbohydr. Polym.* **2011**, *84*, 812.
[7] Kokabi, M.; Sirousazar, M.; Hassan, Z. *Eur. Polym. J.* **2007**, *43*, 773.
[8] Fan, Z.; Liu, B.; Wang, J.; Zhang, S.; Lin, Q.; Gong, P.; Ma, L.; Yang S. *Adv. Funct. Mater.* **2014**, *24*, 3933.
[9] Jin, S. G.; Kim, K. S.; Kim, D. W.; Kim, D. S.; Seo, Y. G.; Go, T. G.; Youn, Y. S.; Kim, J. O.; Yong, C. S.; Choi, H. G. *Int. J. Pharm.* **2016**, *497*, 114.
[10] Shoba, E.; Lakra, R.; Kiran, M. S.; Korrapati, P. S. *RSC Adv.* **2014**, *4*, 60209.
[11] Aytimur, A.; Uslu, İ. *Polym. Plast. Technol. Eng.* **2014**, *53*, 655.
[12] Hasan, A.; Memic, A.; Annabi, N.; Hossain, M.; Paul, A.; Dokmeci, M. R.; Dehghani, F.; Khademhosseini, A. *Acta Biomater.* **2014**, *10*, 11.
[13] Cui, W.; Zhou, Y.; Chang J. *Sci. Tech. Adv. Mater.* **2010**, *11*, 1.
[14] Lee, S.; Kim, J. S.; Chu, H. S.; Kim, G. W.; Won, J. I.; Jang, J. H. *Acta Biomater.* **2011**, *7*, 3868.
[15] Chhabra, H.; Deshpande, R.; Kanitkar, M.; Jaiswal, A.; Kale, V. P.; Bellare, J. R. *RSC Adv.* **2016**, *6*, 1428.
[16] Jin, G.; Prabhakaran, M. P.; Kai, D.; Annamalai, S. K.; Arunachalam, K. D.; Ramakrishna, S. *Biomaterials* **2013**, *34*, 724.
[17] Jannesari, M.; Varshosaz, J.; Morshed, M.; Zamani, M. *Int. J. Nanomed.* **2011**, *6*, 993.
[18] Chen, D. W.; Hsu, Y. H.; Liao, J. Y.; Liu, S. J.; Chen, J. K.; Ueng, S. W. *Int. J. Pharm.* **2012**, *430*, 335.
[19] Shankhwar, N.; Kumar, M.; Mandal, B. B.; Robi, P. S.; Srinivasan, A. *J. Biomater. Sci. Polym. Ed.* **2016**, *27*, 247.
[20] Aytimur, A.; Uslu, I. *Polym. Plast. Technol. Eng.* **2014**, *53*, 655.
[21] Zhang, B.; Lalani, R.; Cheng, F.; Liu, Q.; Liu, L. J. *Biomed. Mater. Res. Part A* **2011**, *99*, 455.
[22] Unnithan, A. R.,; Barakat, N. M.; Pichiah, P. B.; Gnanasekaran, G.; Nirmala, R.; Cha, Y. S.; Jung, C. H.; Newehy, M. E.; Kim, H. Y. *Carbohydr. Polym.* **2012**, *90*, 1786.
[23] Toncheva, A.; Spasova, M.; Paneva, D.; Manolova, N.; Rashkov, I. *Int. J. Polym. Mater. Polym. Biomater.* **2014**, *63*, 657–671.
[24] Zahedi, P.; Rezaeian, I.; Jafari, S. H. *J. Mater. Sci.* **2013**, *48*, 3147.
[25] Karami, Z.; Rezaeian, I.; Zahedi, P.; Abdollahi, M. *J. Appl. Polym. Sci.* **2013**, *129*, 756.
[26] Motealleh, B.; Zahedi, P.; Rezaeian, I.; Moghimi, M.; Abdolghaffari, A. H.; Zarandi, M. A. *J. Biomed. Mater. Res. Part B* **2014**, *102*, 977.
[27] Naseri, N.; Algan, C.; Jacobs, V.; John, M.; Oksman, K.; Mathew, A. P. *Carbohydr. Polym.* **2014**, *09*, 71.
[28] Bonino, C. A.; Krebs, M. D.; Saquing, C. D.; Jeong, S. I.; Shearer, K. L.; Alsberg, E.; Khana, S. A. *Carbohydr. Polym.* **2011**, *85*, 111.
[29] Lee, J.; Tae, G.; Kim, Y. H.; Park, I. S.; Kim, S. H.; Kim, S. H. *Biomaterials* **2008**, *29*, 1872.
[30] Jeong, S. I.; Kim, B. S.; Kang, S. W.; Kwon, J. H.; Lee, Y. M.; Kim, S. H.; Kim, Y. H. *Biomaterials* **2004**, *25*, 5939.
[31] Daranarong, D.; Thapsukhon, B.; Wanandy, N. S.; Molloy, R.; Punyodoma, W.; Fosterb, L. R. *Polym. Int.* **2014**, *63*, 1254.
[32] Su, Y.; Su, Q.; Liu, W.; Lim, M.; Venugopal, J. R.; Mo, X.; Ramakrishna, S.; Al-Deyab, S. S.; EL-Newehy. M. *Acta Biomater.* **2012**, *8*, 763.
[33] Fu, W.; Liu, Z.; Feng, B.; Hu, R.; He, X.; Wang, H.; Yin, M.; Huang, H.; Zhang, H.; Wang, W. *Int. J. Nanomed.* **2014**, *9*, 2335.
[34] Xu, Y.; Wu, J.; Wang, H.; Li, H.; Di, N.; Song, L.; Li, S.; Li, D.; Xiang, Y.; Liu, W.; Mo, X.; Zhou, Q. *Tissue Eng. Part C* **2013**, *19*, 925.
[35] Pokrywczynska, M.; Jundzill, A.; Adamowicz, J.; Kowalczyk, T.; Warda, K. *PLoS One* **2014**, *9*, 105295.
[36] Ramanathan, G.; Singaravelu, S.; Raja, M. D.; Nagiah, N.; Padmapriya, P.; Ruban, K.; Kaveri, K.; Natarajan, T. S.; Sivagnanam, U. T.; Perumal, P. T. *RSC Adv.* **2016**, *6*, 7914.
[37] Qi, P.; Zhou, Y.; Wang, D.; He, Z.; Li, Z. *RSC Adv.* **2015**, *5*, 87180.
[38] Posadowska, U.; Brzychczy-Wloch, M.; Pamula, E. *Acta Bioeng. Biomech.* **2015**, *17*, 41.
[39] Tang, S.; Tian, Bo.; Ke, Q. F.; Zhu, Z. A.; Guo, Y. P. *RSC Adv.* **2014**, *4*, 41500.
[40] Dong, B.; Arnoult, O.; Smith, M. E.; Wnek, G. *Macromol. Rapid Commun.* **2009**, *30*, 539.
[41] Fernández, J.; Etxeberria, A.; Sarasua, J. R. *J. Mech. Behav. Biomed. Mater.* **2012**, *9*, 100.
[42] Kwon, I. K.; Kidoaki, S.; Matsuda, T. *Biomaterials* **2005**, *26*, 3929.
[43] Liu, X.; Lin, T.; Gao, Y.; Xu, Z.; Huang, C.; Yao, G.; Jiang, L.; Tang, Y.; Wang, X. J. *Biomed. Mater. Res. Part B* **2012**, *100*, 1556.
[44] Ong, S. Y.; Wu, J.; Moochhala, S. M.; Tan, M. H.; Lu, J. *Biomaterials* **2008**, *29*, 4323.
[45] Chen, D. W.; Hsu, Y. H.; Liao, J. Y.; Liu, S. J.; Chen, J. K.; Ueng, S. W. *Int. J. Pharm.* **2012**, *430*, 335.
[46] Pascual, A. D.; Vicenteb, A. D. *J. Mater. Chem.* **2016**, *4*, 600.
[47] Shanmugam, K.; Sundaramoorthy, S. *RSC Adv.* **2015**, *5*, 31352.
[48] Gogia, J. S.; Meehan, J. P.; Cesare, P. D; Jamali, A. A. *Semin. Plast. Surg.* **2009**, *23*, 100.
[49] Farndale, R. W.; Sixma, J. J.; Barnes, M. J.; De Groot, P. G. *J. Thromb. Haemost.* **2004**, *2*, 561.
[50] Napavichayanun, S.; Amornsudthiwat, P.; Pienpinijtham, P.; Aramwit, P. *Mater. Sci. Eng. C* **2015**, *55*, 95.
[51] Liua, S. J.; Kau, Y. C.; Chou, C. Y.; Chen, J. K.; Wu, R. C.; Yeh, W. L. *J. Membr. Sci.* **2010**, *355*, 53.
[52] Morgado, P. I.; Lisboa, P. F.; Ribeiro, M. P.; Miguel, S. P.; Simões, P. C.; Correia, I. J.; Ricardo, A. A. *J. Membr. Sci.* **2014**, *469*, 262.